
# Waste of batteries management: Synthesis of magnetocaloric manganite compound from the REEs mixture generated during hydrometallurgical

Sustainable Materials and Technologies 28 (2021) e00267

Contents lists available at ScienceDirect

Sustainable Materials and Technologies

journal homepage: www.elsevier.com/locate/susmat

# Waste of batteries management: Synthesis of magnetocaloric manganite compound from the REEs mixture generated during hydrometallurgical processing of NiMH batteries

Moufida Mansouri [a,*], Francesco Cugini [b,c], Cristian Tunsu [c], Massimo Solzi [b,c], Franca Albertini [c], Burçak Ebin [a], Martina Petranikova [a]

[a] Department of Chemistry and Chemical Engineering, Nuclear Chemistry and Industrial Materials Recycling, Chalmers University of Technology, Gothenburg SE -412 96, Sweden
[b] Department of Mathematical, Physical and Computer Sciences, University of Parma, Parco Area delle Scienze 7/A, 43124 Parma, Italy
[c] IMEM-CNR Institute, Parco Area delle Scienze 37/A, 43124 Parma, Italy

ARTICLE INFO

*Article history:*
Received 21 November 2020
Received in revised form 9 February 2021
Accepted 22 February 2021

*Keywords:*
Rare earth recycling
Ni-MH batteries
Hydrometallurgy
Manganites
Magnetocaloric effect
Magnetic cooling

ABSTRACT

In the present study, rare earth elements (REEs, i.e., La, Ce, Nd, and Pr) were hydrometallurgically recovered in oxalate form with presence of very low concentration of Co, Al, Zn and Ni from solution after processing of spent Nickel metal hydride (Ni-MH) batteries. The recovered mixture was used as alternative source in the synthesis of magnetocaloric materials. In this study, a manganite sample with general formula $ABO_3$ was selected to be prepared since it is relatively easy to synthesize and is tuneable by adjustment of the doping concentration. The conventional solid-state reaction method was used to prepare an orthorhombic structure of manganite with presence of $REE_2O_3$ and $MnO_2$ as secondary phases reported from x-ray pattern at room temperature. The thermomagnetic measurements showed a PM to FM transition at 184 K in a 0.01 T magnetic field that shifts to 194 K by increasing the magnetic field to 1.8 T. The magnetocaloric properties were determined by calculating the isothermal entropy change and directly measuring the adiabatic temperature change. A reversible magnetocaloric effect was observed.



## 1. Introduction

The development of clean energy technologies such as hybrid electric vehicles (HEVs), wind energy, and high-efficiency lighting, catalyst and other related fields has increased the demand for rare earths metals [1]. Rare earths (REEs) consumption is divided between the different sectors as follow: glass industry (polishing, 68%; additives, 42%), 28,400 t; catalysts (fluid cracking, 72%; catalytic converters, 28%), 27,400 t; neodymium-iron boron magnets, 26,300 t; metallurgy and alloys, 23,600 t; and other uses, 23,500 t [1]. However, supply's issues limit such growing consumption. Most of the world's supply comes from only a few sources dominated by China, which controls almost 95% of the global Rare earth oxide production [2]. Therefore, REEs have been considered as a controversial issue and extremely critical raw materials for the European Union that strongly depends on both heavy and light REEs [3]. This poses a potential competition for proposing new solutions including maximizing or optimizing the recovery of REEs from spent nickel metal hydride (Ni-MH) batteries where the anode is commonly a $REENi_5$ alloy consisting of mischmetal (Ce, La, Pr and Nd) and substituents like Co, Ni, Zn, and Al [4–6]. The REE amounts differs from one type of batteries to another. Taking as examples Ni-MH-type, a HEV battery pack contains 3.5 kg REEs [7], 1 g of REEs per AAA battery, 60 g for a household power tool and a hybrid electric vehicle battery contains around 2Kg of REEs [8]. In general, spent batteries are recycled via pyrometallurgy. However, during such treatment, REEs end up in the slag and are not further recovered (e.g. Umicore). Pyrometallurgy have been implemented on an industrial scale by Umicore (Belgium) where the REEs revert to slag phases. The recovery of REEs in molten salt electrolysis was proposed by Honda in collaboration with Japan Metals & Chemicals Co. Ltd. Different methods of extraction have been explored where the REEs are recovered as a mixture [5,9,10]. Compared to other routes, hydrometallurgical processing of NiMH batteries is considered as an environmentally friendly method to bring the REEs mixture into solution feed [11]. The drawback associated with such approach is that the mixed REEs solution has limited industrial use if the contained REEs are not individually separated. Moreover, the separation of such mixture to individual metals is significantly demanding with respect to energy, chemical reagents, and waste generation. Therefore, the reuse of the stream

* Corresponding author.
*E-mail address:* moufida@chalmers.se (M. Mansouri).

https://doi.org/10.1016/j.susmat.2021.e00267

mixture generated from waste of NiMH for synthesis of new materials is challenging and has not been explored yet. The valorisation of REEs mixtures into new applications could improve the recycling rate of those critical raw materials and can make their utilization more sustainable.

An innovative method has been developed for valorisation of waste of batteries. The reuse of the REEs stream is proposed as an alternative source for the synthesis of solid-state refrigerants for magnetic cooling application. In fact, the REEs present in Ni-MH batteries waste are also the main elements composing the magnetocaloric materials with general formula $La_{1-x}REE_xMn_{1-x}M_xO_3$.

The interest in magnetic refrigeration starts with the discovery of the magnetocaloric effect (MCE), which is the change of entropy ($\Delta S_m$) or of temperature ($\Delta T_{ad}$) that accompanies magnetic transitions in materials when a magnetic field is applied or removed, under isothermal or adiabatic condition, respectively. It was firstly discovered in iron by E. Warburg in 1881. The suitability of a magnetocaloric material for cooling application depends on the large and reversible $\Delta S_m$ and $\Delta T_{ad}$ in small field changes and their temperature profile. Another parameter for the evaluation of magnetocaloric effect is the relative cooling power (RCP) which corresponds to the amount of heat transferred between cold and hot sinks in an ideal refrigeration cycle [12].

Thanks to its eco-friendliness and improvements in energy efficiency, magnetic refrigeration is considered as a good alternative for conventional refrigeration based on gas compression/expansion [13,14]. In a typical magnetocaloric refrigerator, a magnetocaloric material is used in the form of a regenerator matrix. An extensive research along this line include the development of new materials and new synthesis methods to search a new environmentally friendly refrigerant. The material selection criteria have been well presented by Gottschall et al. [15]. A wide category of materials have been proposed as candidate for MCE such as Gd based compounds [16,17], $La(FeSi)_{13}$ based alloys [18–20], Mn-Fe-P [21,22], manganites and other compounds [23–26]. Generally, both first order magnetic transition FOMT materials and second order magnetic transition SOMT materials have been studied.

Among the different classes, Lanthanum manganites with general formula $ABO_3$, where A is La and B = Mn were studied as magnetocaloric materials thanks to their near-room-temperature magnetic transition [27]. Recently, Bahl et al. [28] showed that their strength lies in the ability to accurately tune the Curie temperature $T_C$. The tunability of $T_C$ and the magnetocaloric response in a wide temperature range can be achieved by a chemical substitution in A site or B site. REE-elements, such as Ce, Pr, Nd, etc.… were used to substitute La. The effect of substitution on the structural, magnetic and magnetocaloric properties was widely studied [29,30]. The optimization of dopant can improve the magnetocaloric response of these materials. By efficiently REEs and metal site substituting, we can reach the same composition as the virgin compound in the manufacturing process with discarded outputs from recycling of Ni-MH batteries. The mass adoption of REEs magnetocaloric materials is slowed down by the scarcity of REEs. Hence, the use of REEs feed as starting precursors in the synthesis is challenging and motivating.

The main goal of this paper is the valorization of Ni-MH batteries waste by reutilization in the production of magnetocaloric materials. Synthesis, structural and magnetocaloric properties of manganite oxide prepared from Ni-MH wastes were investigated. This approach can support further studies on this topic and it can be considered a more sustainable solution to reduce the waste generated by industries by proposing an application where the waste of batteries can be reused, with a mitigation of the impact related to mining and the dependence on critical raw materials. The proposed solution can help to scale down the economic and environmental impact of the production technologies for magnetocaloric materials.

## 2. Experimental procedure

### 2.1. Materials

Ni-MH batteries, hydrochloric acid (HCl), Cyanex 923 (from Cytec), $NaNO_3$, $HNO_3$ tributyl phosphate diluted (TBP) in kerosene, decanol, oxalic acid (Merck), $Mn(C_2O_4)_3.H_2O$ and ultra-pure water (MilliQ Millipore,> 18 MΩ/cm) were used in this study.

### 2.2. Sample processing

The preparation of the magnetocaloric material from the waste of batteries was done in 2 major steps: REEs recovery from Ni-MH batteries using hydrometallurgical processing and synthesis of manganite starting from the recovered mixture by using solid state reaction.

#### 2.2.1. Hydrometallurgical processing of NiMH: REEs recovery

Solution containing separated REEs from other cathode materials were obtained in the process described by Petranikova et al. [11]. The Ni-MH battery was firstly manually dismantled and pretreated [11]. For leaching, the solid materials were added in smaller amounts at the time (2 g per minute) to 8 M HCl solution at 30°C in 5 L glass leaching reactor.

Then, the extraction was performed by using solvating extractants mainly trialkylphospine oxide mixture Cyanex 923 and tributyl phosphate diluted (TBP) in kerosene in several stages:

- Pre-Extraction: (8% Cyanex 923, 10% TBP, 82% kerosene) was used to remove Fe (99.9%) and Zn (99.9%) from the leachates: the extraction was performed in four extraction stages followed by three scrubbing stages. A low percentage of Co (8%), Y (5%), Mn (1%) and REEs (2%) was co-extracted.
- Main Extraction: (70% Cyanex 923, 10% TBP, 10% kerosene, 10% 1-Decanol) was used to separate Al and REEs from Ni, K and Mg. Three extraction stages were needed. At this stage, 98% Ni, 99.8% K, and 99.5% Mg were obtained in the aqueous phase.
- Scrubbing: Mixture of $NaNO_3$ and $HNO_3$ were used to remove co-extracted Co, Mn and Ni from the organic phases.
- Stripping process:1 M HCl were used to recover Al and REEs. Low impurities of Co, Mn, Ni, Zn and Al were also present in the final product due to high viscosity of the organic phase and entrapment of the aqueous phase from the previous step.

Petranikova et al. [11] showed that seven stages were sufficient to strip out Al and REEs. The process was performed in a counter-current system using pilot plant scale mixer-settlers. The flowsheet of the technology is shown in Fig. 1.

REE ions in solution were precipitated in REE oxalates, $REE_2(C_2O_4)_3$ according to Eq. (1):

$$2\ REE^{3+}{}_{(aq)} + 3\ C_2O_4{}^{2-}{}_{(aq)} \rightarrow REE_2(C_2O_4)_{3(s)} \quad (1)$$

#### 2.2.2. Conventional solid-state reaction method

A polycrystalline sample $REE^*M_xMn_{1-x}O_3$ were prepared by using conventional solid-state reaction method starting from $REE_2(C_2O_4)_3$, $xH_2O$ obtained from the waste and $Mn(C_2O_4)_3.H_2O$. The precursors were mixed in stoichiometric proportions and grinded for 30 min. The obtained powder was then annealed at 800 °C in air for 12 h and pressed into pellets of 15 mm diameter and 2 mm thickness. The pellets were sintered at 900 °C and 1000 °C for 24 h with intermediate grinding and pelleting processes. The final annealing temperature was 1100 °C for 24 h.

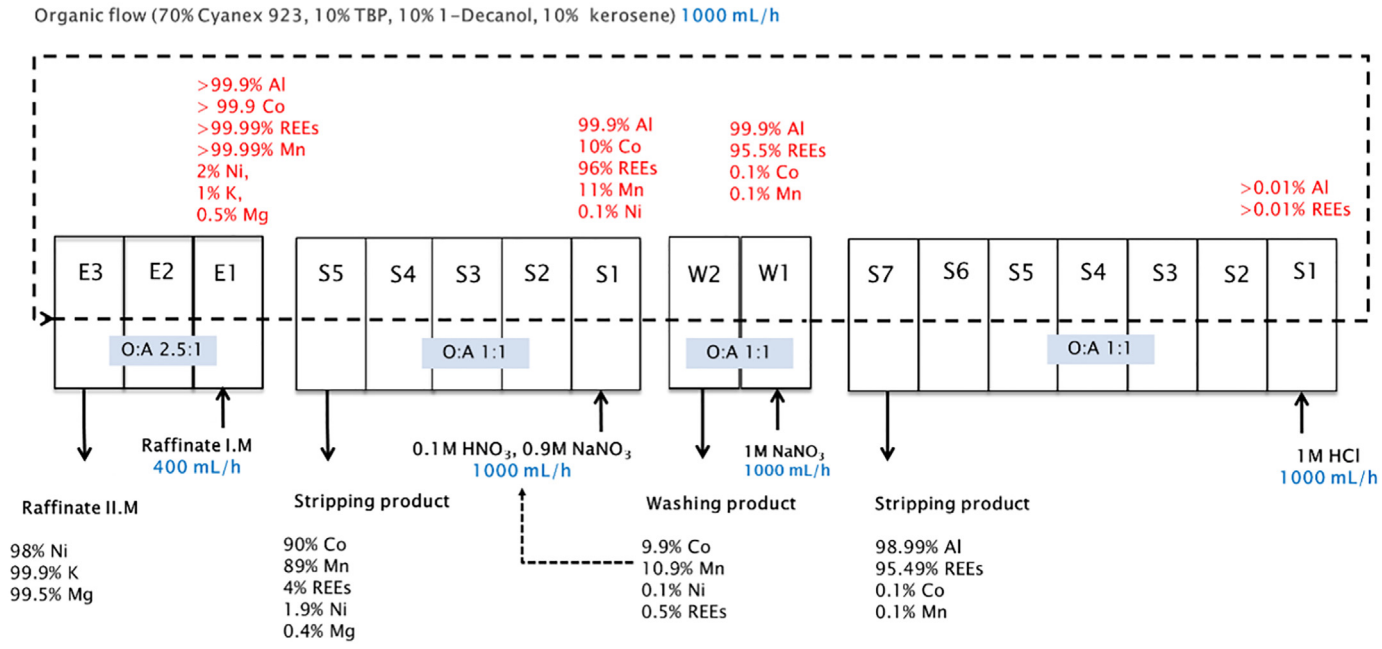


**Fig. 1.** Flow chart of main extraction process for anodic material (using multistage mixer-settler system). Values in red relate to metal in the organic feed after last stage of each step. Values in black relate to metal in the aqueous feed. All the values are reported in regard to the metal concentration in Leachate A. Symbols E, W and S represent extraction, scrubbing and stripping steps respectively [11]).

### 2.3. Characterization

An X-ray diffractometer Bruker (XRD) D8 Advance is used to study the phase structure and purity of the sample. The composition of the rare earth mixture obtained from the waste was determined by an Inductively Coupled Plasma-Optical Emission Spectroscopy (ICP-OES, iCAP 6500, Thermo Fischer). Thermogravimetric analysis was performed to check the decomposition of the oxalate. The chemical composition and the morphology of the recovered waste and manganite sample were studied using scanning electron microscopy (SEM)- JEOL 7800F Prime. Magnetic measurements as a function of temperature in different magnetic fields were performed using an extraction magnetometer (MAGLAB SYSTEM 2000 by Oxford Instruments). The adiabatic temperature change was directly measured with a home-made experimental set up based on a Cernox bare chip temperature sensor [31] with the "cyclic protocol" described in [32]. The field change was achieved by turning on and off a low-inductive electromagnet, with a maximum field of 1.8 T.

## 3. Results and discussion

### 3.1. Structure and morphology

The oxalate was dissolved in HCl and was analyzed with ICP-OES. Its general formula is $REE_2(C_2O_4)_3.\ xH_2O$; REE = $REE^*M_x^*$ where $REE^*$=$La_{0.7}Ce_{0.17}Pr_{0.065}Nd_{0.061}Y_{0.04}Na_{0.004}$ and $M^*_x$ = $Co_{0.0013}Ni_{0.0014}Zn_{0.001}Al_{0.019}Mn_{0.001}$. XRD pattern of oxalate obtained from the waste of NiMH battery powder was presented in Fig. 2(a). The recovery process leads to the formation of $REE_2(C_2O_4)_3.\ xH_2O$ compound which was confirmed by the DIFFRAC.EVA software. The TGA measurement plotted in Fig. 2(b) reports the decomposition temperature of the oxalate. The oxide form $REE_2O_3$ can be obtained by annealing at 900 °C for 12 h (see Fig. 2(c)).

Fig. 3 shows the x-ray diffraction pattern for the prepared manganite compound. The measurement was performed with continuous scanning by a detector covering a 2θ angular range from 10° to 80° with a step size of 0.04 and a wavelength of 1.541874 Å. A composite compound was identified for the manganite by the DIFFRAC.EVA software. It is composed of one major phase of manganite crystallized in orthorhombic structure (81.4%) with presence of two secondary phases that correspond to the REE-oxide mixture (18.00%) used as starting material and $MnO_2$ (0.6%). The phases contents were confirmed by using Match software.

The crystallites size was calculated by using the Debye Scherrer equation:

$$D_{SC} = \frac{K\lambda}{\beta\cos\theta} \quad (2)$$

where K, λ, θ, and $\beta_D$ are respectively the grain shape factor, the x-ray wavelength, the Bragg diffraction angle and the full width at half maximum (FWHM) of the diffraction peak, respectively. The instrumental broadening effect was eliminated. The crystallites size is about 27.87 nm for the manganite sample.

The morphology of the samples was examined with the SEM. The images of the recovered REEs oxalate is observed in Fig. 4. It consists of rods with different diameters ranging from 300 nm to 4 μm and the length of about 500 nm to 10 μm. Micrometric size particles were observed for the manganite compound. The particles are non-homogenous with different shapes. Each particle is composed of different crystallites.

### 3.2. Magnetocaloric study

#### 3.2.1. Magnetometric measurements

Fig. 5(a) reports the temperature dependence of the magnetization M(T) measured in different magnetic fields, ranging from 0.01 T to 1.8 T, with a temperature sweep on heating between 150 and 240 K. The curves show that the sample undergoes a ferromagnetic (FM) to paramagnetic (PM) transition. The critical temperature ($T_C$) was derived by taking the minimum of dM/dT curves (Fig. 5(b)). The inset of the Fig. 5(b) shows the variation of $T_C$ as function of applied magnetic field. The $T_C$ shifts toward higher temperature with the increase of magnetic field indicating an enhancement of the ferromagnetism. The rate

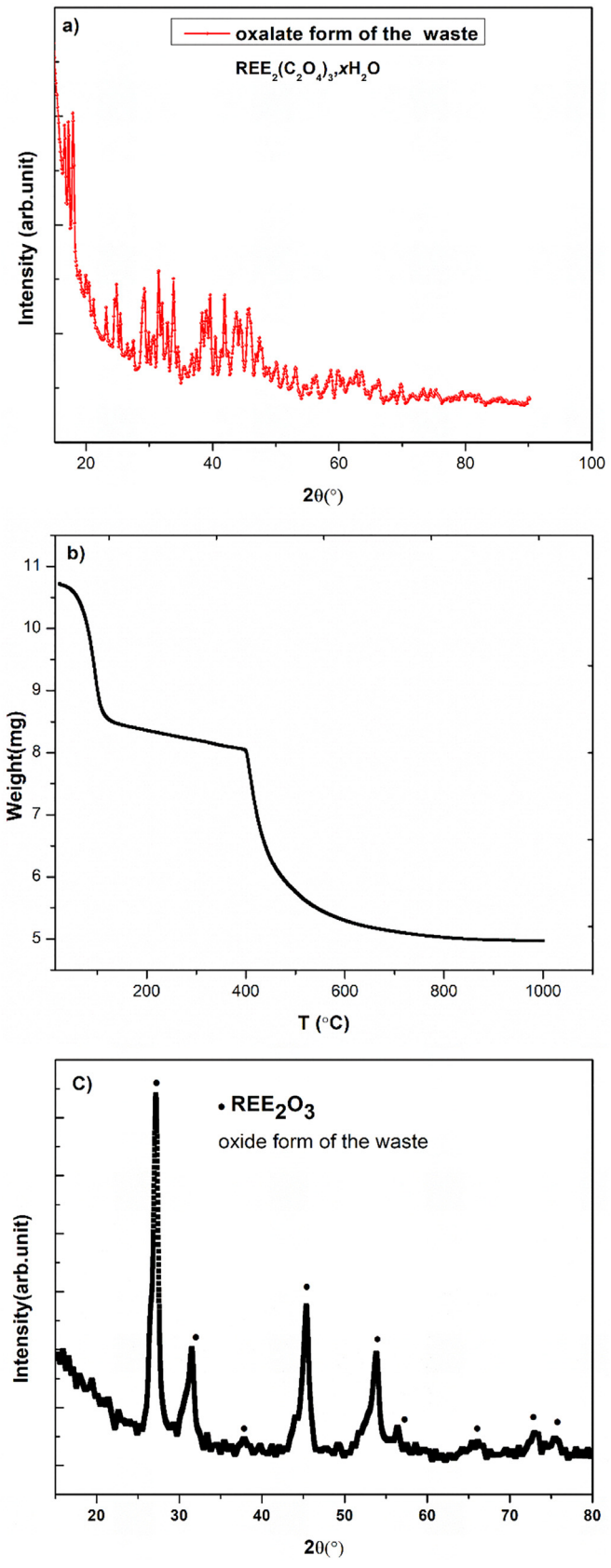


**Fig. 2.** a) X-ray diffraction pattern of the recovered REE-mixture from Ni-MH during hydrometallurgy process, b) Weight loss curves, c) X-ray diffraction pattern of the oxide form of the waste obtained at 900 °C.

of the change is about 5.5 K/T. The $T_C$ varies from 184 ± 1 K to 194 ± 1 K under 0.01 T and 1.8 T respectively. Such behavior was already reported in the literature for different virgin manganites which showed a PM to FM magnetic transition upon cooling [33–37]. The secondary phases do not show magnetic properties in the 100–300 K temperature range, as demonstrated by the absence of other magnetic transitions and the paramagnetic state above the Curie temperature. Their effect is to decrease the net mass magnetization of the prepared material.

Fig. 5(c) shows the temperature dependence of magnetization taken at 0.01 and 1 T on heating and on cooling. No thermal hysteresis between both protocols was detected around the transition in a 0.01 T applied magnetic field, which can be a feature of second order transition of the sample. By increasing the applied magnetic field up to 1 T, no modification was observed on the thermal hysteresis showing no transformation in the phase transition nature. However, the magnetization vs T curves height decreases. Moreover, the magnetization increases from 8.98 $Am^2Kg^{-1}$ to 59 $Am^2Kg^{-1}$.

Additional information on the magnetic properties of the sample can be obtained by studying the inverse of magnetic susceptibility as function of temperature $\chi^{-1}(T)$ at different magnetic fields. The curve $\chi^{-1}(T)$ is plotted in Fig. 5(d). Using the Curie – Weiss (CW) law, $\chi(T) = \frac{C}{T-\theta_p}$, where, C and $\theta_p$ are respectively the Curie constant and the Weiss temperature, we obtained a $\theta_p$ of 187 K. This positive value suggests the presence of ferromagnetic spin interaction. No Griffiths phase like has been detected.

### 3.2.2. Magnetocaloric properties: Isothermal entropy change

The isothermal entropy change $\Delta S_T$ is of central importance for magnetocaloric materials. It is related to the temperature derivative of magnetization M and to the strength of the magnetic field $\mu_0 H$ change through the Maxwell relation:

$$\Delta S_T = \mu_0 \int_0^H \left(\frac{\partial M}{\partial T}\right) dH \tag{3}$$

The $\Delta S_T(T)$ curves for a magnetic field variation of 1 T and 1.8 T, reported in Fig. 6(a), were calculated by applying the Maxwell relation at M(T) data. The maximum entropy change $|\Delta S_T{}^{max}|$ for 1 T is 1.07 ± 0.02 J $kg^{-1}$ $K^{-1}$. By applying a higher magnetic field of 1.8 T, it increases

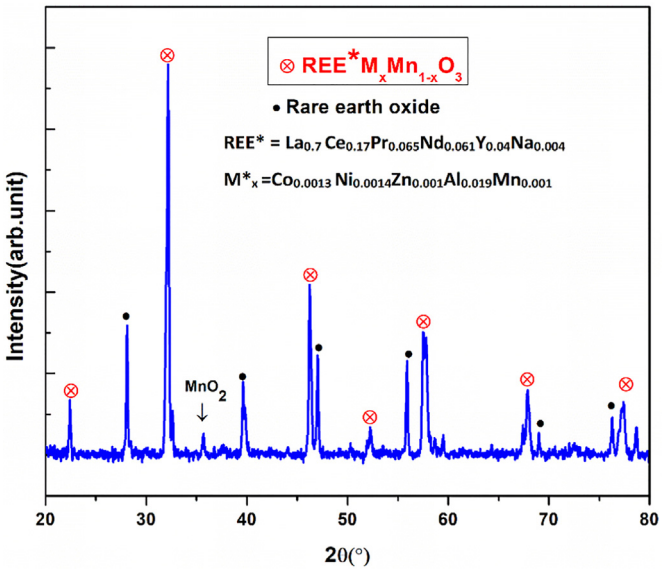


**Fig. 3.** X-ray diffraction pattern of the prepared manganite.

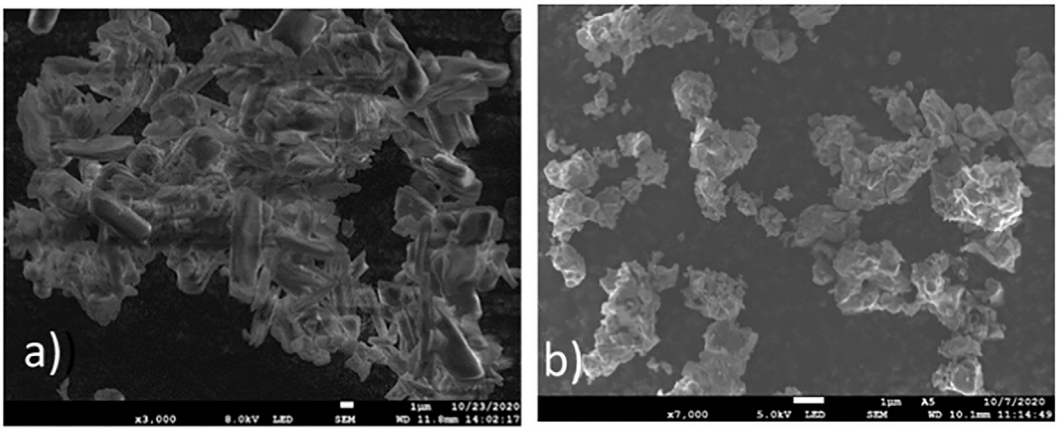


**Fig. 4.** SEM images of a) REEs oxalate recovered from the waste b) manganite sample.

to a value of 1.67 ± 0.05 J $kg^{-1}$ $K^{-1}$. These values are lower compared with the $\Delta S_T$ obtained for other manganite compounds mainly because of the inhomogeneity of the sample and the presence of secondary phases [38–41].

As an example, in recent works, the first order $La_{0.7}Ca_{0.3}MnO_3$ manganite showed a higher entropy change at low magnetic fields. By applying a magnetic field of 0.5 and 1.0 T, it reaches 5.04 and 6.25 J $kg^{-1}$ $K^{-1}$ [42]. This compound shows a higher isothermal entropy, a typical characteristic of first order transition differently from the compound obtained from waste of batteries that shows a second order transition with lower and wider isothermal entropy. We could get the impression that the manganite obtained from waste has a poor

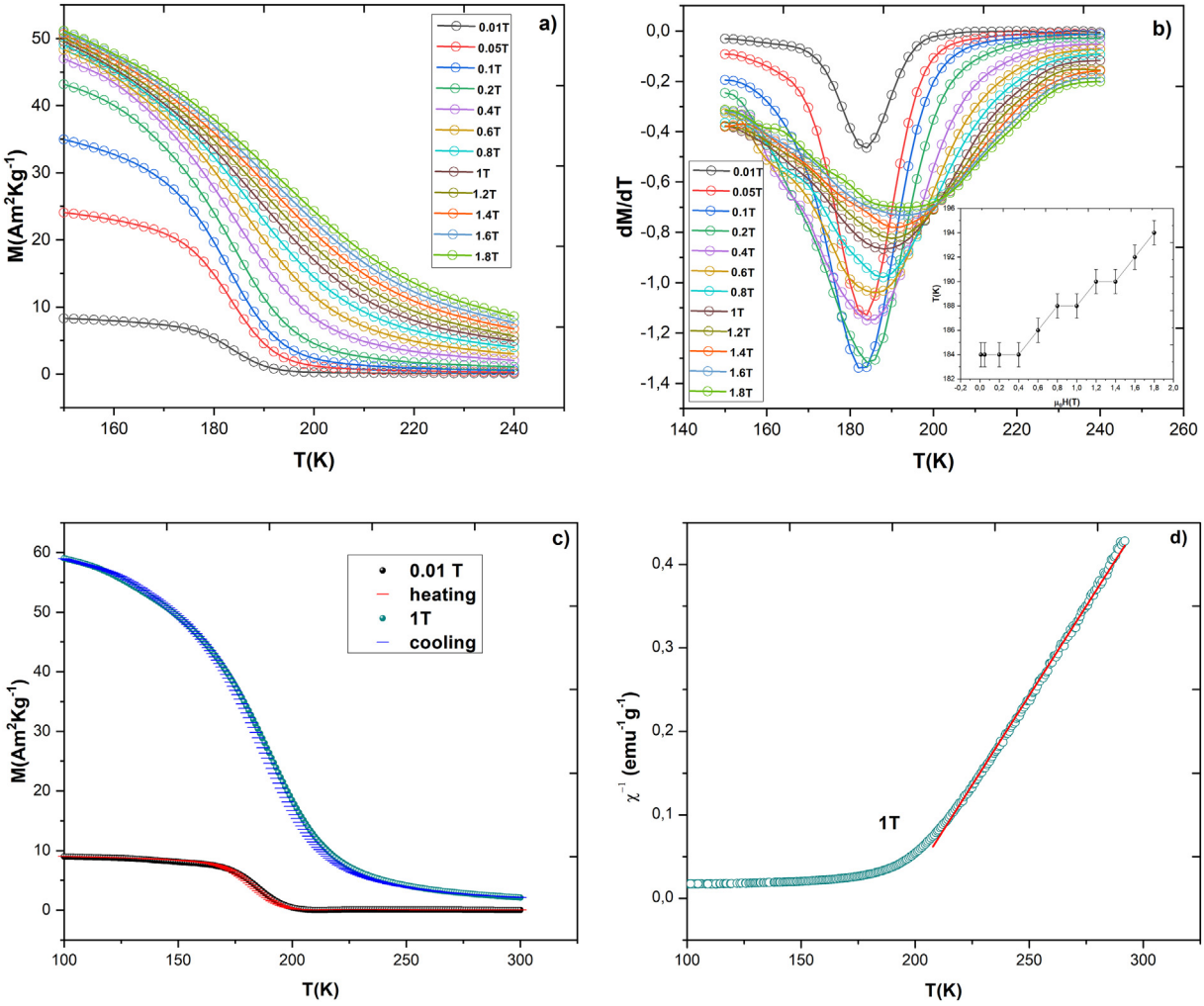


**Fig. 5.** a) Variation of magnetization (M) as function of temperature (T) for the manganite sample in a magnetic field varying from 0.01 T to 1.8 T, b) (dM/dT) versus temperature curves for the manganite sample. The inset shows $T_C$ versus magnetic field curves, c) M(T) curves on heating and cooling for a 0.01 T and 1 T applied magnetic field, d) inverse of susceptibility vs temperature curves for 1 T.

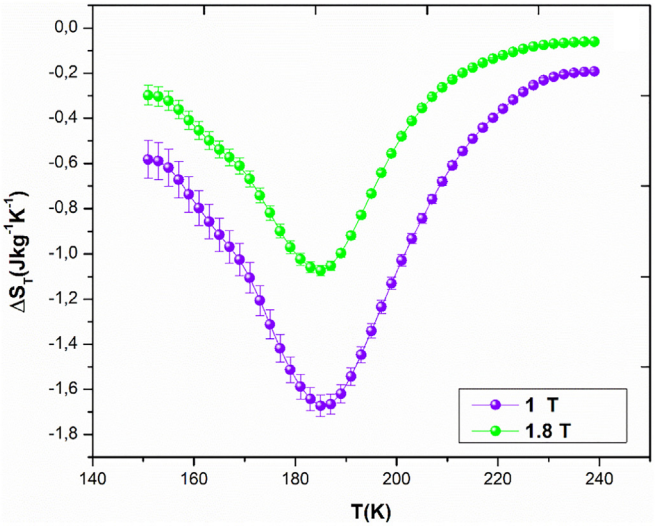


**Fig. 6.** Isothermal entropy change as a function of temperature for two magnetic fields 1 T and 1.8 T variations.

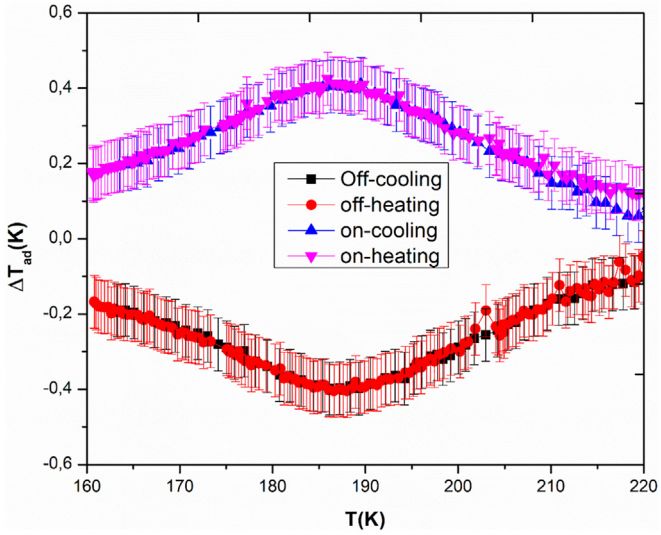


**Fig. 7.** $\Delta T_{ad}(T)$ of the manganite sample directly measured on cooling and on heating by applying and removing a magnetic field of 1.8 T.

performance in comparison to other magnetocaloric compounds. However, it is possible to enhance the MCE performance by exploiting several factors such as composition, grain size, sintering temperature, or pressure application and by improving the homogeneity of the sample. Moreover, combining the obtained manganite from NiMH spent with another manganite composition or oxides can ameliorate the MC feasibility. In a recent work, M. Pekała et al. reported the magnetocaloric properties of the $La_{0.8}Sr_{0.2}MnO_3/La_{0.7}Ca_{0.3}MnO_3$ composite and found that the magnetic field dependence of magnetic entropy change is stronger for the nano- than the polycrysctalline composite [43]. The effect of chemical order on manganite were already reported [44].

The RCP is also an important parameter that can characterize a magnetocaloric material. It can be calculated by considering the magnitude of and their full width at half-maximum $\delta T_{FWHM}$. It is defined as [45]:

$$RCP = \Delta S_{max} * \delta_{FWHM} \quad (4)$$

The values yielded are 37.45 and 78.5 $Jkg^{-1}$ respectively for 1 and 1.8 T. For comparison purpose, the magnetocaloric parameters for studied raw materials that possesses acceptable magnetic cooling properties are presented in Table 1. The sample exhibit comparable performance to other oxides working in a close Curie temperature but very low compared to the intermetallic alloy $La(FeSi)_{13}$ based samples and Gd. The low magnetocaloric parameters values make the present sample not suitable for magnetic cooling application. Further improvement of the compound should be realized.

**Table 1**
Comparison of the magnetocaloric properties for manganite obtained from waste of Ni-MH batteries and other materials studied for magnetic refrigeration.

| Compound | $T_C$ (K) | $\mu_0 H$ (T) | $\Delta T_{ad\text{-}max}$ (K) | $-\Delta S_{max}$ ($Jkg^{-1}\ K^{-1}$) | RCP ($Jkg^{-1}$) | Ref |
|---|---|---|---|---|---|---|
| Manganite from waste of NiMH batteries | 194 | 1.8 | 0.41 | 1.67 | 78.5 | Present work |
| Gd | 299 | 2 | – | 4.2 | 196 | [16] |
| $LaFe_{11.83}Mn_{0.32}Si_{1.3}H_x$ | 294 | 2 | 4.9 | 12.6 | 105.6 | [46] |
| $La_{0.8}Ca_{0.2}MnO_3$ | 183 | 2 | – | 2.23 | 112.36 | [47] |
| $La_{0.7}Sr_{0.3}Mn_{0.9}Ti_{0.1}O_3$ | 210 | 1 | – | 0.84 | 49 | [48] |
| $Sm_{0.35}Pr_{0.2}Sr_{0.45}MnO_3$ | 182.5 | 5 | – | 5.23 | 219.03 | [49] |
| $La_{0.66}Y_{0.04}Ca_{0.3}MnO_3$ | 190 | 2 | – | 5.5 | 143 | [50] |
| $La_{0.4}Pr_{0.3}Ca_{0.3}MnO_3$ | 186 | 5 | – | 6.92 | – | [51] |
| $La_{0.45}Pr_{0.25}Ca_{0.3}MnO_3$ | 199 | 5 | – | 7.27 | – | [51] |

### 3.2.3. Direct measurement of the magnetocaloric effect

The adiabatic temperature change, $\Delta T_{ad}$, is the most important parameter to describe the performance and the feasibility of a magnetocaloric material for cooling application. It is known as the temperature change of the material upon the adiabatic application of magnetic field. It was directly measured using a cyclic protocol that consists in a continuous measurement of the $\Delta T_{ad}$ with a cyclical application of the magnetic field to the material while the temperature of the environment is slowly varied.

The adiabatic temperature change corresponding to the application and removal of a 1.8 T magnetic field upon cooling and heating is plotted in Fig. 7. It shows no thermal hysteresis, as observed in the M (T) curves. The cooling and heating curves are superposed and the measured $\Delta T_{ad}$ is the same both applying and removing the magnetic field, thus demonstrating the reversibility of the magnetocaloric effect. The maximum value is $|\Delta T_{ad}^{max}| = 0.41 \pm 0.07$ K at 198 K upon application and removal of 1.8 T field. This obtained adiabatic temperature change is very low compared to other promising manganite oxide prepared from virgin oxides. This may be due to the presence of different secondary phases such as the REE-oxide mixture and to the broadening of the transition, probably caused by the inhomogeneity of the sample.

The relative cooling power can be also calculated using the following equation [45]:

$$RCP = \Delta T_{ad-max} * \delta_{FWHM} \quad (5)$$

The RCP value obtained from the direct measurement of magnetocaloric effect is $13.53K^2$.

## 4. Conclusion

In conclusion, hydrometallurgy was used as efficient method for the REEs recovery from the outputs generated from Ni-MH batteries. The reuse of the recovered metals for new energy applications was proposed and the synthesis of a manganite sample for magnetic refrigeration application was investigated. The X-ray diffraction structure analysis shows a non-pure manganite phase with the presence of secondary phases; rare earth oxide used as starting material and $MnO_2$. The temperature dependence of magnetization reveals a FM- PM

transition of the sample in the range 184-194 K upon applying a field varying from 0.01 to 1.8 T. The sample showed a reversible magnetocaloric effect, with an isothermal entropy change of 1.67 $Jkg^{-1}\,K^{-1}$ and an adiabatic temperature change of 0.4 K in a magnetic field change of 1.8 T. The magnetocaloric properties are weak compared to different candidates for magnetic refrigeration, mainly because of the inhomogeneity of the sample and the presence of secondary phases. A few future scenarios that can enhance the magnetocaloric efficiency for the waste sample are further A and B site substitutions, producing composite with other materials and changing synthesis conditions. We still found it worthwhile to reuse the waste of Ni-MH batteries for cooling application: the reduction of the oxide form of manganites to an alloy REE($FeSi_{13}$) may give better chance for this application.

## Author statement

Investigation, visualization, writing—original draft preparation, M.M.; conceptualization, methodology, validation, writing—review and editing, M.M., F.C., C.T., M.S., F.A., B.E., M.P.; supervision and project administration, M.P.; All authors have read and agreed to the published version of the manuscript.

## Declaration of Competing Interest

The authors declare that there is no conflict of interest.

## Acknowledgment

This research was supported by FORMAS (Grant No: 2017-00637) and ÅForsk (Grant No: 16-406).

## References

[1] T.G. Goonan, S. Geological, Rare Earth Elements: End Use and Recyclability, DOI 2011.
[2] K. Binnemans, P.T. Jones, T. Müller, L. Yurramendi, Rare earths and the balance problem: how to Deal with changing markets? J. Sustain. Metall. 4 (2018) 126–146.
[3] S. British Geological, M. Bureau de Recherches Géologiques et, S. Deloitte, C. European, I.E. Directorate-General for Internal Market, Smes, o. Toegepast natuurwetenschappelijk, Study on the review of the list of critical raw materials: final report, 2017.
[4] T. Müller, B. Friedrich, Development of a recycling process for nickel-metal hydride batteries, POWER J. Power Sour. 158 (2006) 1498–1509.
[5] K. Korkmaz, M. Alemrajabi, Å. Rasmuson, K. Forsberg, Recoveries of valuable metals from spent nickel metal hydride vehicle batteries via sulfation, selective roasting, and water leaching, J. Sustain. Metall. 4 (2018) 313–325.
[6] B. Ebin, M. Petranikova, C. Ekberg, Physical separation, mechanical enrichment and recycling-oriented characterization of spent NiMH batteries, J Mater Cycles Waste Manag 20 (2018) 2018–2027.
[7] J. Yano, T. Muroi, S.I. Sakai, Rare earth element recovery potentials from end-of-life hybrid electric vehicle components in 2010-2030, J. Mater. Cycles Waste Manage. 18 (2016) 655–664.
[8] A. United States Environmental Protection, Rare Earth Elements: A Review of Production, Processing, Recycling, and Associated Environmental Issues, DOI 2012.
[9] M.S. Gasser, M.I. Aly, Separation and recovery of rare earth elements from spent nickel-metal-hydride batteries using synthetic adsorbent, MINPRO Int. J. Min. Proc. 121 (2013) 31–38.
[10] S. Maroufi, R.K. Nekouei, R. Hossain, M. Assefi, V. Sahajwalla, Recovery of Rare Earth (i.e., La, Ce, Nd, and Pr) Oxides from End-of-Life Ni-MH Battery via Thermal Isolation, ACS Sust. Chem. Eng. 6 (2018) 11811–11818.
[11] M. Petranikova, I. Herdzik-Koniecko, B.-M. Steenari, C. Ekberg, Hydrometallurgical processes for recovery of valuable and critical metals from spent car NiMH batteries optimized in a pilot plant scale, HYDROM Hydrometall. 171 (2017) 128–141.
[12] K.A. Gschneidner, V.K. Pecharsky, MAGNETOCALORIC materials, Annu. Rev. Mater. Sci. 30 (2000) 387.
[13] N.H. Dung, Z.Q. Ou, L. Caron, L. Zhang, D.T. Thanh, G.A. de Wijs, R.A. de Groot, K.H. Buschow, E. Brck, Mixed magnetism for refrigeration and energy conversion, Adv. Energy Mater. 1 (2011) 1215–1219.
[14] E. Bruck, Developments in magnetocaloric refrigeration, J. Phys. D. Appl. Phys. 38 (2005) R381.
[15] T. Gottschall, K.P. Skokov, M. Fries, A. Taubel, I. Radulov, F. Scheibel, D. Benke, S. Riegg, O. Gutfleisch, Making a cool choice: the materials library of magnetic refrigeration, AENM Adv. Energy Mater. 9 (2019).
[16] V.K. Pecharsky, K.A. Gschneidner Jr., Giant magnetocaloric effect in $Gd_5(Si_2Ge_2)$, Phys. Rev. Lett. 78 (1997) 4494.
[17] V.K. Pecharsky, K.A. Gschneidner, Tunable magnetic regenerator alloys with a giant magnetocaloric effect for magnetic refrigeration from 20 to 290K, Appl. Phys. Lett. 70 (1997) 3299–3301.
[18] O. Gutfleisch, A. Yan, K.H. Muller, Large magnetocaloric effect in melt-spun $LaFe_{13-x}Si_x$, J. Appl. Phys. 97 (2005) 10M305.
[19] A. Fujita, S. Fujieda, Y. Hasegawa, K. Fukamichi, Itinerant-electron metamagnetic transition and large magnetocaloric effects in $La(Fe_xSi_{1-x})_{13}$ compounds and their hydrides, Phys. Rev. B 67 (2003) 104416.
[20] J. Lyubina, O. Gutfleisch, M.D. Kuz'min, M. Richter, La(Fe,Si)13-based magnetic refrigerants obtained by novel processing routes, J. Magn. Magn. Mater. 320 (2008) 2252–2258.
[21] F. Guillou, G. Porcari, H. Yibole, N. van Dijk, E. Brück, Taming the first-order transition in giant magnetocaloric materials, Adv. Mater. 26 (2014) 2671–2675.
[22] H. Yibole, F. Guillou, L. Zhang, N.H. van Dijk, E. Brück, Direct measurement of the magnetocaloric effect in MnFe(P,X)(X= As, Ge, Si) materials, J. Phys. D. Appl. Phys. 47 (2014) 075002.
[23] H. Zhao, J. Xia, D. Yin, M. Luo, C. Yan, Y. Du, Rare earth incorporated electrode materials for advanced energy storage, Coord. Chem. Rev. 390 (2019) 32–49.
[24] D. Yang, Y. Liu, H. Jiang, M. Liao, N. Qu, T. Han, Z. Lai, J. Zhu, A novel FeCrNiAlTi-based high entropy alloy strengthened by refined grains, J. Alloys Compd. 823 (2020) 153729.
[25] L. Li, P. Xu, S. Ye, Y. Li, G. Liu, D. Huo, M. Yan, Magnetic properties and excellent cryogenic magnetocaloric performances in B-site ordered $RE_2ZnMnO_6$ (RE = Gd, Dy and Ho) perovskites, Acta Mater. 194 (2020) 354–365.
[26] Y. Zhang, D. Guo, B. Wu, H. Wang, R. Guan, X. Li, Z. Ren, Magnetic properties and magneto-caloric performances in $RECo_2B_2C$ (RE = Gd, Tb and Dy) compounds, J. Alloys Compd. 817 (2020) 152780.
[27] S.L.A.R. Dinesen, S. Morup, Direct and indirect measurement of the magnetocaloric effect in $La_{(0.67)}Ca_{(0.33-x)}Sr_{(x)}MnO_{(3\pm\delta)}$ (x [0;0.33]), J. Phys. Condensed Matter 17 (2005) 6257–6269.
[28] C.R.H. Bahl, D. Velazquez, K.K. Nielsen, K. Engelbrecht, K.B. Andersen, R. Bulatova, N. Pryds, High performance magnetocaloric perovskites for magnetic refrigeration (3 pages), Appl. Phys. Lett. 100 (2012) 121905.
[29] M.-H. Phan, S.-C. Yu, Review of the magnetocaloric effect in manganite materials, MAGMA J. Mag. Mag. Mater. 308 (2007) 325–340.
[30] M.S. Anwar, F. Ahmed, B. Heun Koo, Influence of Ce addition on the structural, magnetic, and magnetocaloric properties in $La_{0.7-x}Ce_xSr_{0.3}MnO_3$ (0x0.3) ceramic compound, Ceramics Int. 41 (2015) 5821–5829.
[31] G. Porcari, M. Buzzi, F. Cugini, R. Pellicelli, C. Pernechele, L. Caron, E. Brück, M. Solzi, Direct magnetocaloric characterization and simulation of thermomagnetic cycles, Rev. Sci. Instrum. 84 (2013) 073907.
[32] F. Cugini, M. Solzi, On the direct measurement of the adiabatic temperature change of magnetocaloric materials, J. Appl. Phys. 127 (2020) 123901.
[33] A. Rostamnejadi, M. Venkatesan, P. Kameli, H. Salamati, J.M.D. Coey, Magnetocaloric effect in $La_{0.67}Sr_{0.33}MnO_3$ manganite above room temperature, J. Magn. Magn. Mater. 323 (2011) 2214–2218.
[34] M. Abassi, Z. Mohamed, J. Dhahri, E.K. Hlil, Theoretical investigations on the magnetocaloric and electrical properties of a perovskite manganite $La_{0.67}Ba_{0.1}Ca_{0.23}MnO_3$, Dalton Trans. 45 (2016) 4736–4746.
[35] S. Othmani, M. Bejar, E. Dhahri, E.K. Hlil, The effect of the annealing temperature on the structural and magnetic properties of the manganites compounds, J. Alloys Compd. 475 (2009) 46–50.
[36] J. Makni-Chakroun, R. M'Nassri, W. Cheikhrouhou-Koubaa, M. Koubaa, N. Chniba-Boudjada, A. Cheikhrouhou, Effect of A-site deficiency on investigation of structural, magnetic and magnetocaloric behaviors for (LaSr)-lacunar manganites, Chem. Phys. Lett. 707 (2018) 61–70.
[37] M. Zarifi, P. Kameli, M. Mansouri, H. Ahmadvand, H. Salamati, Magnetocaloric effect and critical behavior in $La_{0.8-x}Pr_xSr_{0.2}MnO_3$ (x = 0.2, 0.4, 0.5) manganites, Solid State Commun. 262 (2017) 20–28.
[38] F. Guillou, H. Yibole, G. Porcari, L. Zhang, N.H.V. Dijk, E. Brück, Magnetocaloric effect, cyclability and coefficient of refrigerant performance in the MnFe(P, Si, B) system, J. Appl. Phys. 116 (2014) 063903.
[39] R. Skini, S. Ghorai, P. Ström, S. Ivanov, D. Primetzhofer, P. Svedlindh, Large room temperature relative cooling power in $La_{0.5}Pr_{0.2}Ca_{0.1}Sr_{0.2}MnO_3$, J. Alloys Compd. 827 (2020) 2020–2006.
[40] K. Fukamichi, A. Fujita, S. Fujieda, Large magnetocaloric effects and thermal transport properties of $La(FeSi)_{13}$ and their hydrides, J. Alloys Compd. 408-412 (2006) 307–312.
[41] R. Bjørk, C.R.H. Bahl, M. Katter, Magnetocaloric properties of $LaFe_{13-x-y}Co_xSi_y$ and commercial grade Gd, J. Magn. Magn. Mater. 322 (2010) 3882–3888.
[42] A.N. Ulyanov, J.S. Kim, G.M. Shin, Y.M. Kang, S.I. Yoo, Giant magnetic entropy change in $La_{0.7}Ca_{0.3}MnO_3$ in low magnetic field, J. Phys. D. Appl. Phys. 40 (2006) 123–126.
[43] M. Pękała, K. Pękała, V. Drozd, K. Staszkiewicz, J.-F. Fagnard, P. Vanderbemden, Magnetocaloric and transport study of poly- and nanocrystalline composite manganites $La_{0.7}Ca_{0.3}MnO_3/La_{0.8}Sr_{0.2}MnO_3$, J. Appl. Phys. 112 (2012) 023906.
[44] J.S. Amaral, P.B. Tavares, M.S. Reis, J.P. Araújo, T.M. Mendonça, V.S. Amaral, J.M. Vieira, The effect of chemical distribution on the magnetocaloric effect: a case study in second-order phase transition manganites, J. Non-Cryst. Solids 354 (2008) 5301–5303.
[45] K.A. Gschneidner, V.K. Pecharsky, A.O. Tsokol, Recent developments in magnetocaloric materials, Rep. Prog. Phys. 68 (2005) 1479–1539.
[46] K. Morrison, K.G. Sandeman, L.F. Cohen, C.P. Sasso, V. Basso, A. Barcza, M. Katter, J.D. Moore, K.P. Skokov, O. Gutfleisch, Evaluation of the reliability of the measurement of key magnetocaloric properties: A round robin study of $La(Fe,Si,Mn)H_\delta$ conducted by the SSEEC consortium of European laboratories, Int. J. Refrig. 35 (2012) 1528–1536.

[47] M. Wali, R. Skini, M. Khlifi, E. Dhahri, E.K. Hlil, A giant magnetocaloric effect with a tunable temperature transition close to room temperature in Na-deficient $La_{0.8}Na_{0.2-x}\square_xMnO_3$ manganites, Dalton Trans. 44 (2015) 12796–12803.
[48] S. Kallel, N. Kallel, O. Peña, M. Oumezzine, Large magnetocaloric effect in Ti-modified $La_{0.70}Sr_{0.30}MnO_3$ perovskite, Mater. Lett. 64 (2010) 1045–1048.
[49] A. Mleiki, S. Othmani, W. Cheikhrouhou-Koubaa, M. Koubaa, A. Cheikhrouhou, E.K. Hlil, Effect of praseodymium doping on the structural, magnetic and magnetocaloric properties of $Sm_{0.55-x}Pr_xSr_{0.45}MnO_3$ ($0.1 \leqslant x \leqslant 0.4$) manganites, J. Alloys Compd. 645 (2015) 559–565.
[50] T.-L. Phan, T.A. Ho, T.V. Manh, N.T. Dang, C.U. Jung, B.W. Lee, T.D. Thanh, Y-doped $La_{0.7}Ca_{0.3}MnO_3$ manganites exhibiting a large magnetocaloric effect and the cross-over of first-order and second-order phase transitions, J. Appl. Phys. 118 (2015) 143902.
[51] A. Rebello, V.B. Naik, R. Mahendiran, Large reversible magnetocaloric effect in $La_{0.7-x}Pr_xCa_{0.3}MnO_3$, J. Appl. Phys. 110 (2011) 013906.